Proposed method to estimate the liquid-vapor accommodation coefficient based on experimental sonoluminescence data

Gabriela F. Puente[1] and Fabián J. Bonetto[1,2]
[1]*Instituto Balseiro/UNCu, Laboratorio de Cavitacion y Biotecnologia, 8400-San Carlos de Bariloche, Argentina*
[2]*CNEA-CONICET, 8400-San Carlos de Bariloche, Argentina*
(Received 26 August 2003; revised manuscript received 15 November 2004; published 31 May 2005)

We used the temporal evolution of the bubble radius in single-bubble sonoluminescence to estimate the water liquid-vapor accommodation coefficient. The rapid changes in the bubble radius that occur during the bubble collapse and rebounds are a function of the actual value of the accommodation coefficient. We selected bubble radius measurements obtained from two different experimental techniques in conjunction with a robust parameter estimation strategy and we obtained that for water at room temperature the mass accommodation coefficient is in the confidence interval [0.217,0.329].

DOI: 10.1103/PhysRevE.71.056309 PACS number(s): 78.60.Mq, 47.55.Bx

The value of the liquid-vapor accommodation coefficient affects such diverse phenomena as water droplet nucleation and growth in the atmosphere, heterogeneous boiling through microlayer evaporation, and bubble dome condensation and velocity of bubble collapse in cavitation among others.

The accommodation coefficient may be the limiting factor for the energy concentration in bubble luminescence phenomena. In single-bubble sonoluminescence (SBSL) the vapor that is present inside the bubble limits the maximum compression that can be obtained. The noble gases present in the bubble could achieve higher temperatures if it were not for the quenching effect of the water vapor. Several endothermic reactions occur at temperatures of the order of 5000 K (around 0.5 eV) that absorb energy and prevent the noble gases from becoming hotter [1]. A larger accommodation coefficient implies a smaller amount of water vapor inside the bubble at the moment of maximum compression and therefore a greater concentration of energy.

Inside the bubble we distinguish between gas, which is noncondensable for the temperature range of interest, and vapor, which corresponds to the same chemical species as the liquid. In this paper the vapor is water vapor and gas corresponds to air.

During the bubble compression of the gas-vapor mixture, the vapor partial pressure inside the bubble is higher than the saturation pressure corresponding to the bubble wall temperature. Nonequilibrium condensation occurs under these circumstances. This is the key element we take advantage of to estimate the accommodation coefficient. The evaporation rate and the condensation rate [2], (also Yasui, [1]) at the liquid-vapor interface can be expressed as

$$\dot{m}_{\mathrm{eva}} = \frac{\alpha_M}{(2\pi R_v)^{1/2}} \frac{p_v^*}{T_{L,i}^{1/2}} \tag{1}$$

$$\dot{m}_{\mathrm{con}} = \frac{\alpha_M}{(2\pi R_v)^{1/2}} \frac{\Gamma p_v}{T_B^{1/2}},$$

$$\dot{m} = \dot{m}_{\mathrm{eva}} - \dot{m}_{\mathrm{con}}, \tag{2}$$

where α_M is the accommodation coefficient for evaporation and condensation, R_v is the gas constant for water vapor, p_v^* is the saturation vapor pressure at the temperature of the liquid at the bubble wall $T_{L,i}$, T_B is the mixture temperature at the bubble wall, and p_v is the actual vapor partial pressure inside the bubble. Γ is [1]

$$\Gamma = \exp(-\Omega^2) - \Omega\sqrt{\pi}\left(1 - \frac{2}{\sqrt{\pi}}\int_0^{\Omega} \exp(-x^2)dx\right), \tag{3}$$

$$\Omega = \frac{\dot{m}}{p_v}\left(\frac{R_v T}{2}\right)^{1/2},$$

where T is the bubble temperature.

Direct experimental results for the accommodation coefficient are not common in the literature. For example a recent compilation of these results [3] contains two entries for water and they are for ice and vapor but no data are presented for water liquid-vapor. In the literature researchers have used values that differ by several orders of magnitude, from $\alpha = 10^{-3}$ up to 1 [4].

In this work we compute the temporal evolution of the radius of a SBSL bubble using the Keller-Miksis version of the Rayleigh-Plesset equation and conservation equations that take into account heat and mass transfer. The equations have the accommodation coefficient α_M as a free parameter. From the solution we identified the temporal intervals that have the strongest dependency on α_M. We combine these numerical results with experimental results and a robust parameter estimation technique to obtain α_M.

In particular we consider a sonoluminescent bubble undergoing nonlinear oscillations in an acoustic field with frequency $f \approx 30$ kHz and acoustic pressure amplitude $p_a \approx 1.4$ bar(1 bar = 10^5 Pa) and static pressure $p_0 = 1$ bar. The resonator is spherical and has a diameter of $d \approx 60$ mm. The resonator is filled with water, there are no free surfaces (closed resonator), and the water has a concentration of air $c_\infty/c_0 \approx 0.2$ or Ar $c_\infty/c_0 \approx 2\times10^{-3}$, where c_0 is the air (or Ar) saturation concentration in water at a pres-

sure p_0. The exact values we use depend on the experiments but they do not depart significantly from the ones given in this paragraph.

We describe first the particular form of the thermofluid dynamic equations used in this work. A number of versions of the Rayleigh-Plesset-Prosperetti (RPP) [4] equations have been used to study the temporal evolution of a SBSL bubble's radius. One of the most common is presented by Barber [5]. Brenner *et al.* [4] and Prosperetti *et al.* [6] presented a generalized RPP equation that includes the one in [4] as a particular case. We used in this work the following RPP equation [1]:

$$\left(1-\frac{\dot{R}}{c}+\frac{\dot{m}}{c\rho_L}\right)R\ddot{R}+\frac{3}{2}\dot{R}^2\left(1-\frac{\dot{R}}{3c}+\frac{2\dot{m}}{3c\rho_L}\right)$$
$$=\frac{1}{\rho_L}\left(1+\frac{\dot{R}}{c}\right)\left[p_B-p_s\left(t+\frac{R}{c}\right)-p_\infty\right]$$
$$+\frac{\ddot{m}R}{\rho_L}\left(1-\frac{\dot{R}}{c}+\frac{\dot{m}}{c\rho_L}\right)+\frac{\dot{m}}{\rho_L}\left(\dot{R}+\frac{\dot{m}}{2\rho_L}+\frac{\dot{m}\dot{R}}{2c\rho_L}\right)$$
$$+\frac{R}{c\rho_L}\frac{dp_B}{dt}, \tag{4}$$

where R is the bubble radius, c is the speed of sound in the liquid, $p_B(t)$ is the pressure of the liquid on the external side of the bubble wall, $p_s(t)$ is a nonconstant ambient pressure component such as a sound field, and p_∞ is the undisturbed pressure. $p_B(t)$ is related to the pressure inside the bubble by [1]

$$p_B(t)=p_t(t)-\frac{2\sigma}{R}-\frac{4\mu}{R}\left(\dot{R}-\frac{\dot{m}}{\rho_L}\right)-\dot{m}^2\left(\frac{1}{\rho_L}-\frac{1}{\rho_g}\right) \tag{5}$$

where σ is the surface tension, μ is the liquid viscosity, ρ_L is the liquid density, and ρ_g is the density inside the bubble.

Equation (4) corresponds to the general RPP equation in [4] with $\lambda=0$ (Keller-Miksis equation).

We assume that the bubble interior is a homogeneous mixture of (water) vapor molecules and gas atoms. We also consider that the carrier gas (O_2 or air in our case) dissolved in the water does not remain inside the bubble due to chemical reactions occurring when the bubble interior is at high temperature (Lohse *et al.* [7]). The mixture is considered to be a van der Waals gas with all properties being weighted averages using the number of particles (molecules or atoms depending on the case) [1]. The heat transfer equation is as in [1,8]. Based on previous work ([Toegel *et al.* [9], Storey and Szeri [10]) we assumed the mass transfer to be controlled by binary mass diffusion during the 50 ns previous to collapse. During these 50 ns prior to collapse $R(t)$ does not provide information to obtain α_M. This lack of information introduces an uncertainty in the modeling. We incorporated this modeling uncertainty into the experimental uncertainty.

We numerically solved the resulting system of ordinary differential equations using a Runge-Kutta-Fehlberg scheme with adaptive time step. Figure 1 shows the results of $R(t)$ for different α_M. We observe that the resulting $R(t)$ is a strong function of α_M for small α_M but the curves do not change much for $\alpha_M > 0.1$.

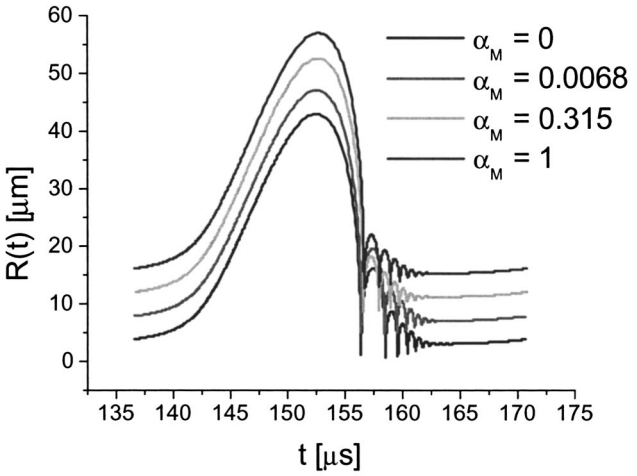

FIG. 1. Temporal evolution of the bubble radius for different accommodation coefficients in the range 0 through 1. The larger the accommodation coefficient, the larger the maximum radius and the longer time of collapse. It can be seen that the maximum radius after collapse is not monotonically varying with the accommodation coefficient. The accommodation coefficient equal to 0.315 corresponds to the largest maximum radius after collapse among the values shown in this figure.

This initial value problem required the amount of gas atoms present in the bubble to be known. Usually the number of gas atoms in the bubble is given in terms of R_0^g, the radius that a gas bubble with the same number of atoms would have at reference (typically ambient) pressure and temperature. However, in the experiments, one does not control R_0^g directly. Instead one controls the gas concentration in the liquid c_∞. The system pressure and temperature determine c_0. The condition for no net gas mass flow in one cycle for a pure Ar bubble is [10]

$$\frac{c_\infty}{c_0}=\int_0^T p_g R^4(t')dt' \Big/ \int_0^T R^4(t')dt' \tag{6}$$

where $R(t)$ is the bubble radius and p_g is the partial pressure of the gas (Fig. 2).

The problem as defined is not strictly an initial value problem because R_0^g is not known in advance and Eq. (6) is not necessarily satisfied. We added a bisection subroutine (shooting method) to compute R_0^g until Eq. (6) was satisfied. With this procedure we obtained a fixed point of the problem, the condition $d(c_\infty/c_0)/dR_0^g > 0$ taken at constant p_a assured that the equilibrium was stable [7]. For the range of parameters that we analyzed there was a single stable solution (Fig. 2).

We compare the results of our model with the more sophisticated model of Storey [11] (Fig. 3), who performed a direct numerical simulation for the same problem. The overall agreement is good. The damping of the rebounds is captured by our simpler and computationally less expensive model.

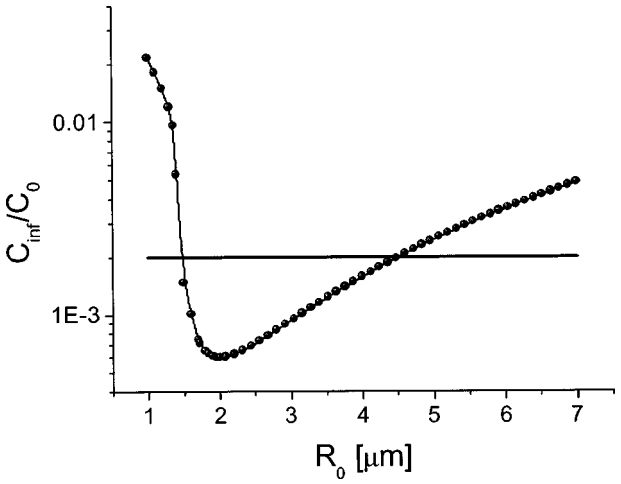

FIG. 2. Plot of $\int_0^T R^4 p_t dt / \int_0^T R^4 dt$ as a function of the argon ambient radius of the bubble for an acoustic pressure amplitude of $p_a = 1.396$ bars. For $p_a = 1.396$ bars the diffusively stable bubble radius is $R_0^g = 4.53$ μm. The fixed point $R_0^g = 1.50$ μm is diffusively unstable.

Based on the numerical results we identified the basic selection criteria for the experimental data to be used. Time intervals where the bubble radius evolved slowly are more representative of thermodynamical equilibrium than nonequilibrium evaporation or condensation. These time intervals did not contain relevant information regarding the α_M. For our estimation procedure it was necessary to use experimental results that resolve the $R(t)$ fastest temporal scales, exact values of the relative maximum values during the rebounds, or both.

It was also necessary to determine the bubble radius with a pure experimental technique (i.e., not using a RP equation fit). An experimental technique that satisfied both requirements is based on a Laser-Doppler velocimeter for a SBSL bubble [Fig. 5(a)] below [12]. The best technique to resolve the $R(t)$ fastest temporal scales is based on femtosecond pulses illuminating the bubble at repetition rates of the order

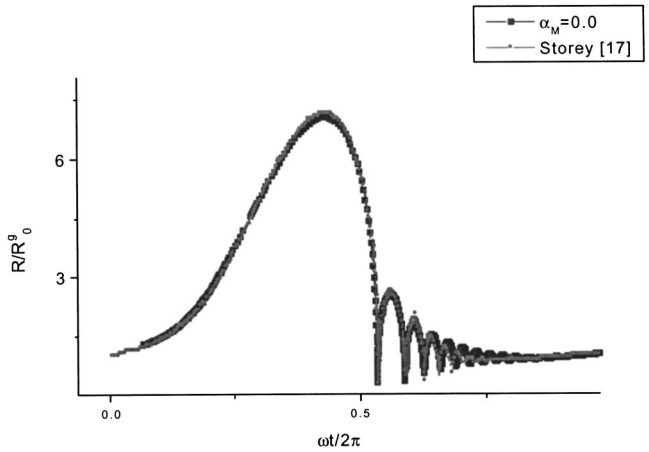

FIG. 3. Comparison between our model results with $\alpha_M = 0$ and the direct numerical simulation (DNS) results of Storey [17] for the same conditions. Our simpler model captures the damping in the rebounds very well.

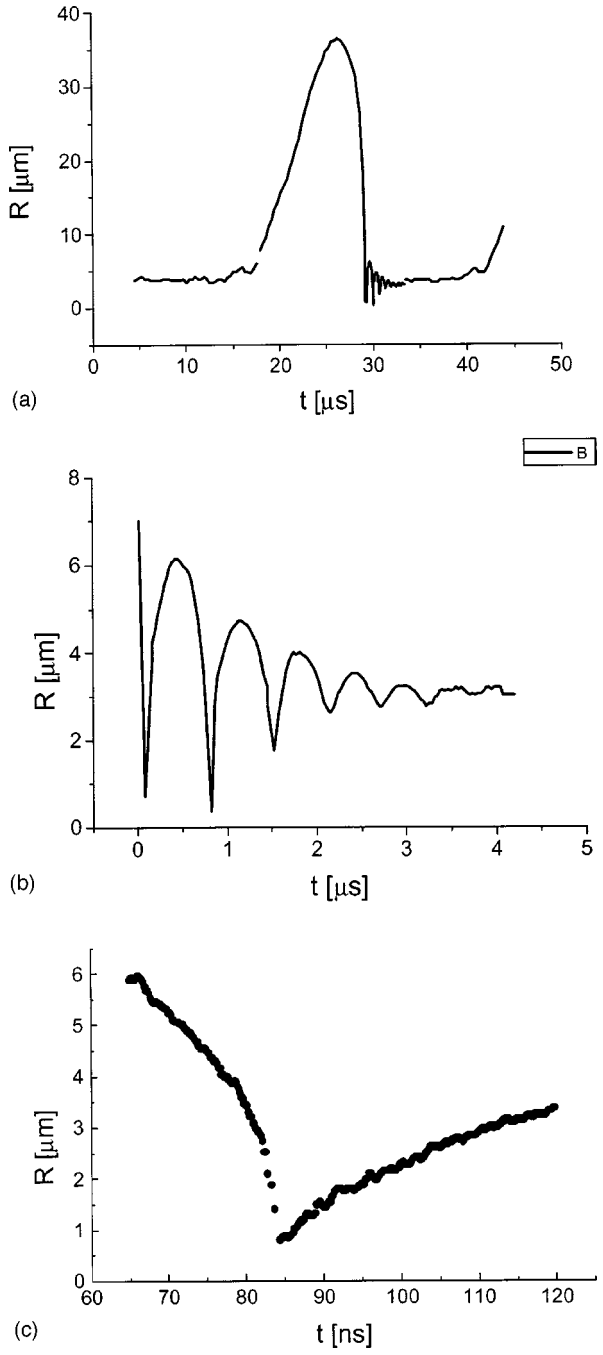

FIG. 4. Experimental bubble radius R as a function of time for $c_\infty / c_0 = 0.002$ (corresponding to Fig. 15 in [7]). (a) corresponds to a whole bubble cycle measured with the standard [9] Mie scattering technique. (b) corresponds to the measurement of the rebounds region only. (c) was obtained using a pulsed Ti:sapphire laser Mie scattering technique.

of 76 MHz [Fig. 4(a) [13]]. However, in this case the determination of the absolute value of the velocity requires a RP fit.

The vast majority of $R(t)$ estimations were measured illuminating a bubble with a continuous wave (cw) laser and locating a phototube (or photomultiplier tube) near the Brewster angle (83° from forward for the water-gas system). The scattered light was collected with a large aperture lens to

increase the signal to noise ratio and to reduce the amplitude of the Mie resonances. Mie theory for the scattering of light predicts a smooth quadratic relationship between scattered light and bubble radius in this configuration. The voltage measured (which is proportional to the light intensity) depends on the bubble radius as in

$$V = a_0 + a_2 R^2,$$

where a_0 corresponds to the signal for the limit $R = 0$ and has three contributions: an average value (which can be estimated and removed), a rms value (that comes from electromagnetic noise and laser intensity fluctuation if the water is not extremely pure), and stray light from reflections and/or refractions that may change with time. Most researchers estimate a_2 (and p_a) using oversimplified Rayleigh-Plesset equations (e.g., without considering water vapor inside the bubble). This strategy introduces an unacceptable error for this paper.

The results obtained in this manner are useful for several purposes. However, they are not adequate for this work. An error propagation analysis performed on a_0 concludes that very small changes in a_0 produce large changes in the minimum radius and the maximum compression and expansion velocities. The information that is useful to estimate α_M is contained in these time intervals.

The other condition we used to select the data was to use $R(t)$ corresponding to the minimum possible amount of gas in the bubble. The gas reduces the mass flow at the interface and ideally one would like to have no gas in the bubble. However, there are no reported sonoluminescence bubble conditions without some small amount of noble gases.

Figures 4 and 5 show the $R(t)$ for the experimental techniques mentioned above. Figure 4(a) was obtained with the femtosecond laser pulse technique [13]. The inset [Fig. 4(b)] around the first collapse shows the region of maximum velocities and the rebounds. Figure 4(c) shows the main collapse. Figure 5(b) shows the velocities measured with the laser-Doppler technique [12]. The inset [Fig. 5(a)] shows the reconstructed radius as a function of time obtained from the integration of the velocity measurements.

We used χ^2 minimization of key values obtained from the experimental data for the parameter estimation. These values were the absolute maximum radius and relative maximum radii (during the rebounds), minimum radius during the main collapse and relative minimum radii (during the rebounds), time location of radius extrema, the phase with respect to the acoustic pressure excitation, and maximum and minimum velocities. All times are measured with respect to the time of collapse. We call these N quantities experimentally obtained $a_1,\ldots,a_N$. We call the corresponding computed quantities $b_1(p_1,\ldots,p_M),\ldots,b_N(p_1,\ldots,p_M)$ where $p_1,\ldots,p_M$ are the parameters to be estimated. In our case $M=2$, p_1 is α_M and p_2 is p_a. We define the random variable χ^2 [14]

$$\chi^2 = \sum_{i=1}^{N} [a_i - b_i(p_1,\ldots,p_M)]^2/\sigma_i^2 \qquad (7)$$

where σ_i is the standard deviation (we took them to be the estimated experimental errors) of the random variables a_i. If

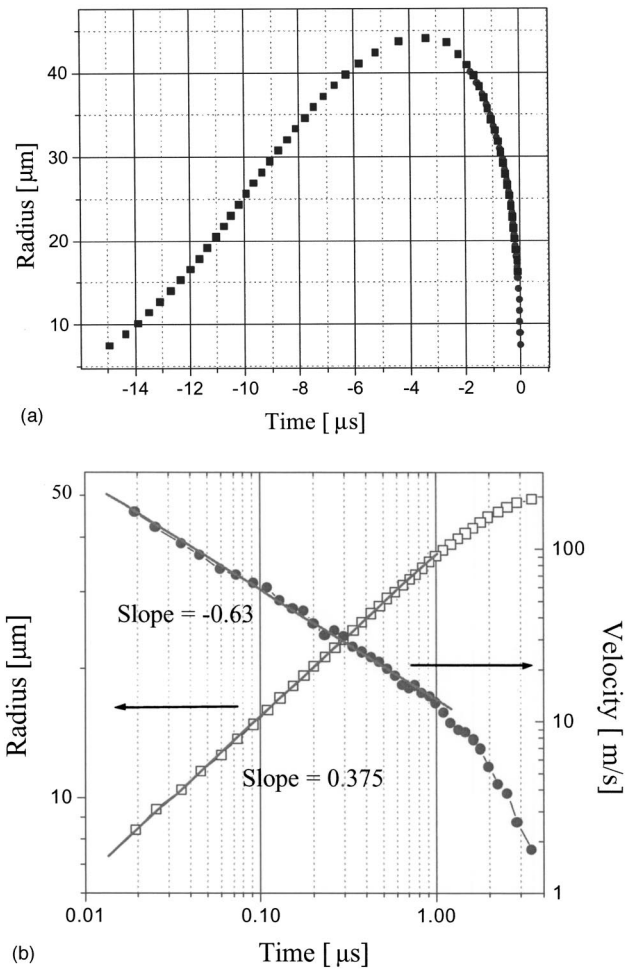

FIG. 5. Experimental bubble radius R as a function of time for $c_\infty/c_0=0.002$ (Delgadino and Bonetto [12]). (a) corresponds to a bubble radius cycle measured with the laser-Doppler technique. (b) corresponds to the radius and velocity measurements during the main collapse. Note the logarithmic scale on the time axis and the y axis. Also the independent variable in this plot is the time of collapse t_c minus the time t.

the a_i's are normal (Gaussian) distributions and the b_i's are the mean values of the a_i's then each term in Eq. (7) corresponds to a Gaussian distribution with p_i mean and standard deviation of 1. In this case χ^2 defined in Eq. (7) has a χ^2 distribution with N degrees of freedom. Estimating the parameters $p_1,\ldots,p_M$ from χ^2 minimization is also a maximum likelihood estimator. Our free parameters for all experiments were α_M and p_a and thus $M=2$.

We define a new variable that is measured with respect to the minimum condition $\Delta\chi^2=\chi^2-\chi^2_{\min}$. With this definition $\Delta\chi^2$ is a random variable with a χ^2 distribution with $N-M$ degrees of freedom. We must keep in mind that the a_i's are not normally distributed. For one thing the radii are always positive; also the time intervals can only be positive the way we define them. However, we can still use Eq. (7) for the parameter estimation even though it is not a maximum likelihood estimator under these conditions.

Figure 6 shows a plot of $\Delta\chi^2$ for the experimental results shown in Fig. 5 as a function of one of the parameters

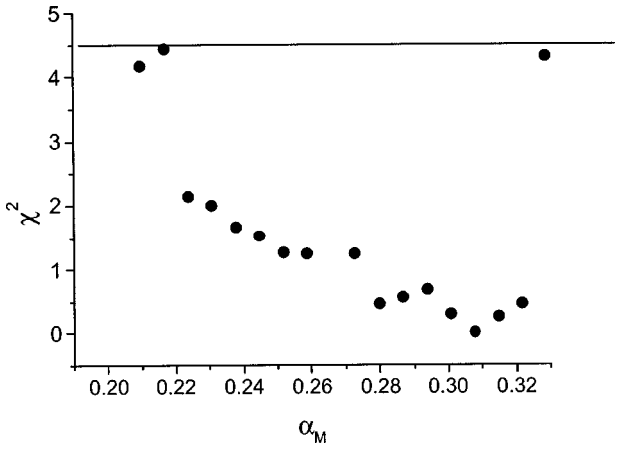

FIG. 6. Plot of $\Delta\chi^2$ as a function of the accommodation coefficient α_M for an acoustic pressure amplitude $p_a=1.369$ for the data shown in Fig. 5. The $\Delta\chi^2$ minimum (equal to 0 by definition) corresponds to $\alpha_1=0.315$ and $p_a=1.369$ bars. The confidence intervals are obtained through a projection of the $\Delta\chi^2=4.7$ isocurve to the corresponding axis.

(α_M) to be estimated with the other already estimated (p_a). $\Delta\chi^2=0$ corresponds to $p_a=1.396$ bars and $\alpha_M=0.308$. For this case the degrees of freedom are $N-M=4$ and using a probability $p=0.68$ the resulting value for χ^2 is 4.5. Thus the value for p_a is 1.396 ± 0.02 bar and the value for α_M from this experimental set is in the confidence interval $\alpha_M \in [0.217, 0.329]$.

We studied how sensitive the presented confidence interval results were to the model assumptions. In particular we may question the Toegel approach to the solution of the mass boundary layer. The size of the boundary layer is obtained based on dimensional analysis so it may be a factor of 2 or 0.5 off. We computed the α_M that minimized the χ^2 for a factor 1 (the base case), a factor 2, and a factor 0.5, obtaining α_M equal to 0.308, 0.275, and 0.329, respectively. We could see that the variation is much smaller than the length of the confidence interval (0.112). We concluded that this assumption did not affect our estimated results significantly.

Two theoretical and numerical calculations of the accommodation coefficient have been made to our knowledge obtaining dissimilar results. Matsumoto [15] performed molecular dynamics simulations at the liquid-vapor interface and obtained for water the value $\alpha_M=0.35$ for a temperature of 350 K. Leighton [16] computed the accommodation coefficient based on classical statistical mechanics, obtaining a value of $\alpha_M=0.00667$.

We used the data in Fig. 4 to compute the $\Delta\chi^2$ corresponding to $\alpha_M=0.006\,67$ and 0.35. We obtained $\Delta\chi^2=270.19$ and 8.45, respectively. For this experimental dataset the degrees of freedom were $N-M=7$. With a $p=0.68$ the value for $\Delta\chi^2$ is 8.5. Thus it is very unlikely that the value $\alpha_M=0.006\,67$ is correct. The value $\alpha_M=0.35$ is inside the confidence interval. The confidence interval is large due to the fact that the experiment was conducted in such a way that no absolute measurements in the radii (and therefore the velocities) were performed. The use of relative radii extrema and velocity did not differentiate the results for $\alpha_M>0.2$.

We believe that the approach presented in this paper could be used to estimate the accommodation coefficient for any liquid-vapor combination that is compatible with an acoustically levitated bubble. We know that we require for this purpose some small amount of a noble gas. Using small amounts of noble gases leads to a more accurate estimation of the accommodation coefficient. We conclude also that the temporal regions of thermodynamic nonequilibrium are the most important to be measured in order to estimate the accommodation coefficient. The gas-vapor temperatures are very high during bubble collapse. However, the liquid temperature at the bubble wall is very close to room temperature as reported by Kamath *et al.* With the method proposed here we estimate a single effective accommodation coefficient. The underlying assumption is that the α_M is a function of the liquid temperature and a weak function of the vapor temperature.

We thank Raúl Urteaga for helpful comments. We acknowledge the technical support of Sebastian Eckardt and Daniel Mateos. G.F.P. is financed by Anpcyt/Secyt. The partial support of Foncyt/Anpcyt/Secyt through Grant No. PICT 12-09848 is gratefully appreciated.

[1] K. Yasui, Phys. Rev. E **56**, 6750 (1998).
[2] M. Volmer, *Kinetik der Phasebildung* (Steinkopff, Dresden 1939).
[3] Y. V. Polezhaev and N. V. Pavlyukevich, in *International Enc. of Heat and Mass Transfer*, edited by G. F. Hewitt *et al.* (CRC Press, New York, 1997).
[4] M. P. Brenner *et al.*, Rev. Mod. Phys. **74**, 425 (2002).
[5] B. P. Barber, Phys. Rep. **281**, 65 (1997).
[6] A. Prosperetti *et al.*, J. Acoust. Soc. Am. **83**, 502 (1988).
[7] M. P. Lohse *et al.*, Phys. Rev. Lett. **76**, 1158 (1996).
[8] Y. Hao and A. Prosperetti, Phys. Fluids **11**, 1309 (1999).
[9] R. S. Toegel *et al.*, Phys. Rev. Lett. **84**, 2509 (2000); **88**, 034301 (2002).
[10] B. D. Storey and A. J. Szeri, J. Fluid Mech. **396**, 203 (1999).
[11] B. D. Storey, Phys. Rev. E **64**, 017301 (2001).
[12] G. A. Delgadino and F. J. Bonetto, Phys. Rev. E **56**, R6248 (1997); G. A. Delgadino, Ph.D. thesis, Rensselaer Polytechnic Institute, 1998; G. A. Delgadino *et al.*, Chem. Eng. Commun. **189**, 786 (2002).
[13] K. R. Weninger *et al.*, Phys. Rev. Lett. **78**, 1799 (1997); F. J. Bonetto and P. Carrica (unpublished).
[14] B. Efron and R. Tibshirani, Stat. Sci., **1**, 54 (1986).
[15] M. Matsumoto (private communication to Yasui in Ref. [5]).
[16] T. G. Leighton, *The Acoustic Bubble* (Pergamon Press, Oxford, 1996).
[17] B. D. Storey, Phys. Rev. E **64**, 017301 (2001).